

NATIONAL ADVISORY COMMITTEE FOR AERONAUTICS

No. 1013

RECORDING RAPIDLY CHANGING CYLINDER-WALL TEMPERATURES

By Adolf Meier

Forschung auf dem Gebiete des Ingenieurwesens
Vol. 10, No. 1, January-February 1939

Washington
May 1942

3 1176 01325 7747

NATIONAL ADVISORY COMMITTEE FOR AERONAUTICS

TECHNICAL MEMORANDUM NO. 1013

RECORDING RAPIDLY CHANGING CYLINDER-WALL TEMPERATURES*

By Adolf Meier

SUMMARY

The present report deals with the design and testing of a measuring plug suggested by H. Pfriem for recording quasi-stationary cylinder wall temperatures. The new device is a resistance thermometer, the temperature-susceptible part of which consists of a gold coating applied by evaporation under high vacuum and electrolytically strengthened. This resistance layer, being located on the surface of the wall, enables an immediate surface temperature reading not obtainable heretofore with the conventional thermocouples. Its inertia is negligible. The uncertain and tedious conversion of the test data to the surface is eliminated. A further advantage over the thermocouple lies in the much higher current fluctuations which permit the charting of the temperature curve without amplification. The new method combines substantially higher instrumental accuracy with a maximum of simplicity in operation. Eventual correction of test data is greatly simplified by the laminated structure of the measuring plug.

After overcoming initial difficulties, calibration of plugs up to and beyond 400°C was possible. The measurements were made on high-speed internal combustion engines.

The increasing effect of the carbon deposit at the wall surface with increasing operating period is indicated by means of charts.

*"Messung schnellveränderlicher Zylinderwandtemperaturen."
Forschung auf dem Gebiete des Ingenieurwesens, vol.
10, no. 1, Jan.-Feb. 1939, pp. 41-54.

I. INTRODUCTION

In spite of the great importance attached to the heat transfer in reciprocal engines between working medium and cylinder wall, the experiments up to now have been restricted to the study in slow-speed engines. The measurement in high-speed engines had been impeded by the inadequacy of the conventional method of recording the quasi-stationary wall temperature from which the heat exchange between working medium and cylinder wall is easiest to obtain. In view of the present trend toward high revolution speeds in all reciprocal engines it seemed desirable to develop a new test method which permits the recording of rapidly changing wall temperatures.

In all such experiments, the use of thermocouples has become practically standard practice. But their greatest drawback consisted in the fact that the temperature distribution could be recorded only at a certain distance below the surface which, in addition, was dependent upon frequency and phase of the individual harmonics. This introduced an uncertainty in the recording of the higher harmonics, since the damping of the temperature oscillation penetrating in the wall increases considerably with ascending frequency up to the test station. It also made necessary a harmonic analysis of the measured temperature oscillation and a conversion of the individual harmonics after correction for amplitude and phase to the surface. In addition, the complicated structure of the test point, the dissimilarity of the chemical values of the employed materials, and the effect of the occurring short-circuit currents made an accurate assessment of the produced temperature field impossible, which in turn precluded an exact prediction of the correction factors. (A critical study of the sources of errors in the measurement of rapidly changing surface temperatures by means of thermocouples can be found in an article by H. Pfriem. (See reference 1.)

A further drawback of the conventional thermocouple is its low thermoelectric force of about 0.05 millivolt per °C. Since the oscillation amplitudes of the wall temperature, especially on high-speed engines, are low, the thermovoltage changes are insufficient for the indicating devices suitable for recording rapidly changing voltage fluctuations, and therefore must be amplified by thermionic valves which, aside from being very inconvenient,

introduce new sources of errors. And in addition, the statistic fluctuations of the electronic current of the first valve are disturbingly perceptible and set a limit to the instrumental accuracy.

II. DESCRIPTION OF MEASURING PLUG

The new plug is a resistance thermometer, not a thermocouple (fig. 1). It consists of a metallic, slightly tapered plug element Stk with a central hole. Its length equals that of the wall thickness into which it is to be installed so that it is flush with it. The end facing the operating room carries an electrically insulating layer I on to which a very thin layer of gold W is evaporated and acts as resistance. A wire D_1 , one end of which is connected to the resistance layer and leads outside, is cemented into the hole, the sides of which are also coated with an insulating layer I. The other end of the resistance layer is located at point A on the plug element where a second wire D_2 is attached.

As is seen, the temperature responsive part lies at the surface, hence registers its temperature directly. The corrections of the test data likely to be necessary because of installation disturbance of the test plug are much easier to apply, as it can be approximately dealt with as stratified body.

A further advantage lies in the much higher voltage changes which can easily be raised to 100 times the thermovoltage fluctuations. Thus, the disturbing fluctuations in the transmission level of the first thermionic valve remain ineffective. But, in general, such valve amplification will be unnecessary, as a sensitive oscillograph loop itself permits the direct recording of the temperature oscillations.

III. PLUG DESIGN

1. Material

The use of any heat-resisting, electrically insulating substance, as plug element material, was ruled out because of machining difficulties. On the other hand, the

insulating layer under the resistance layer must be of the same over-all thickness and its total area in intimate contact with the base metal in order to insure uniform heat conduction without local overheating.

As suggested by Pfriem, aluminum was to be used because it lends itself readily as base for the resistance layer by electrolytic oxidation Eloxal process.. The oxide layer is very solidly joined to the base metal, since it itself is of the same metal. The experiments were so satisfactory that no other metal was tried out..

Pure aluminum as well as any other electrolytically oxidizable aluminum alloy is suitable (for instance: Al-Mg, Al-Mg-Mn, Al-Mg-Si quoted in German Standard Specifications DIN 1713). Hard drawn kinds are preferable because of better machinability. The lead-in wires were commercial aluminum products.

In the choice of resistance metal only noble metals came into question. But silver was ruled out because of the danger of sulfite formation, particularly for measurements in combustion engines; platinum, because of its catalytic properties. The gold used in the tests proved entirely satisfactory in every respect.

2. Electrolytic Oxidation of Plug

This Eloxal process is so well known that no detailed description is necessary. But one fundamental difficulty is pointed out. It required many experiments and the utmost care to assure a satisfactory connection between the centrally cemented wire and the resistance layer. A good contact must be without the least joint, because the extremely thin resistance layer cannot bridge it or even fill it. The use of aluminum as wire was therefore dictated; because with wire and plug element of the same heat expansion coefficient any gaps are safely avoided during heating..

Experience indicates that the properties of electrolytically produced aluminum oxide deposits change within certain limits by suitably chosen processing conditions. When oxidized with direct current the layers are generally very hard and mechanically extremely resistant, but very soft and elastic with alternating current. Hence the

coating in the hole housing the cemented wire is preferably applied with direct current. But hard Eloxal layers are unsuitable as insulating base of the resistance layer because of their tendency to develop hair cracks at temperatures above 150°C which destroy the resistance layer. As shown in figure 1 the hole facing the operating room - termed the front hereafter - is slightly conically countersunk.

Before the Eloxal treatment of the hole, all surfaces which were not to be oxidized were given a protective coating against the effect of the bath. The current was supplied through the wire soldered or riveted into the plug element. The great scattering ability of the bath admits of a satisfactory coating even in the hole.

The bath consisted of a 4-percent aqueous solution of oxalic acid. The current density was 20 ma/cm^2 , the duration of the oxidizing process was 2.5 hours.

The central lead-in wire is conically flattened at its cemented end to match the tapered flare in the plug element. This assumed a clean fit free from cement or gaps. Following the cementing of the wire the highly polished front of the plug was electrolytically oxidized with alternating current for 1.5 hours at the same current density. The obtained deposit was about 0.02 mm. Figure 2 shows the transition from the frontal area of the wire (light portion) over the Eloxal coating of the hole to the plug element before application of resistance layer (magnified a hundred times).

3. Resistance Layer

In order to assure maximum instrumental accuracy the resistance of the gold film must be adapted to the particular test method. Direct measurements require low resistance values; the use of amplifiers, high, as subsequent considerations will prove.

The step nearest at hand would be to change the layer resistance through the precipitated gold and herewith the layer thickness. Assuming 100 times the distance of two molecule layers as smallest possible thickness so as to sufficiently remain without the range of irregular conductivity, the resistance at an evenly gilded front would still

be too low even by direct measurement. This fact alone dictates a higher resistance of the layer applied by means of a pattern in suitable form.

After various attempts with zigzag-shape patterns (the plug elements had two wire passages then) the use of spiral patterns, and specifically, balance springs such as used in pocket watches finally proved particularly suitable. This gives the layer the form of a spirally wound strip. And plugs of the smallest dimensions can be obtained without any difficulty, because balance springs of any required size are commercially available.

To branch the current from the resistance layer to the plug element, the edge is broken at any desired spot and the base metal exposed (fig. 1). The apparatus developed for depositing the gold film is sketched in figure 3. It consists of a spherical glass flask with the evaporating device mounted in the neck of the flask. The gold is placed in the form of fine gold wire in the tungsten spiral W , which, after evacuation of the apparatus, is electrically heated to at least 10^{-4} millimeter mercury column. To assure adhesion of the pattern Sch (balance spring) to the plug surface to be gilded, the plug St was damped between the poles of a small magnet M_1 during the process. The curved distribution of the lines of force held the balance spring to the base. In order to prevent the formation of shadows incidental to the 0.5-millimeter high pattern, it was necessary to have either the plug or the tungsten spiral rotate. The latter was found to be preferable. The spiral was attached at the lower end of a shaft with horizontal axis (fig. 3), the heating current being supplied by way of slip rings and slip-ring brushes. The upper end of the shaft carries an armature A which rotates in the field of a magnet system M_2 placed externally around the neck of the flask and consists of three radial magnets set at 120° to one another, by means of which a rotating field is produced. The ground, closed glass tube attached below at the flask is merely intended to receive the long wires of the plug and to afford easy removal of any gold wire dropped occasionally from the tungsten spiral as a result of inattention.

The structure of the metallic layers deposited under high vacuum differs, in general, very markedly from that of the compact metal. This is evidenced, on the one hand by the lack of cohesion, whence the coats can be readily

wiped off, and on the other, by the structural change in time. However, this change is attended by a rise in the electric conductivity, which prevents the immediate use of a thinly deposited metal layer as resistance. This unusual behavior has been the subject of a number of experiments. (A detailed report on the present state of progress concerning the electrical conductivity and structure of thinly deposited metal coatings with a comprehensive list of references will be found in reference 2.) The cause is traceable to the extremely fine crystalline structure typical of the precipitated layers and its tendency to form larger crystals. By briefly heating to about 150°C , the layer can be solidly anchored to the base as a result of more rapid crystal growth. The aging of the layer can be accelerated by heat but not satisfactorily. In figure 4 the time rate of resistance drop in a precipitated layer at constant temperature of 200°C is illustrated, the time coordinate being plotted in hyperbolic scale to emphasize the high rate of change at the start. The curve is indicative of a marked falling off of resistance until it reaches the limiting value. Frequently repeated plug calibrations would therefore become necessary.

The investigation of the test plug further disclosed a change in the Eloxal layer. The attempts to reach maximum temperatures were invariably followed by destruction of the precipitated layer at around 400°C . Diffusion of the gold in the Eloxal layer which would be effectively aided by the high temperature seemed, however, improbable, because the destruction occurred only on alternating-current layers, but not on direct-current layers. It rather seems to confirm the widely held opinion that the alternating-current layers consist of alumina at least near the surface, but not the direct-current layers. The change of hydroxide to oxide, which starts at around 400° , would explain the mechanical destruction of the layer. Eloxal layers heated to 400° before deposition of the gold film manifested the same behavior on heating after the layer had been deposited. This fact is suggestive of a reconversion of oxide by water absorption during cooling.

The destruction could be avoided as soon as the gold was electrolytically deposited onto the evaporated layer, because the strengthened layer was resistant enough. But, at the same time, the aging of the deposited part progressed so far, as a result of the addition of a much more distinct crystal lattice, that no further resistance decrease took place after 1 hour heating of the plug at 400° ,

even by repeated calibration. The electrolytical strengthening of the layer further enabled the reduction of the layer resistance to the desired amount. An electrolytically strengthened gold deposit is shown in figure 5.

The calibration curve of a plug is reproduced in figure 6. The almost linear aspect is very advantageous for instrumental purposes. The mean temperature coefficient obtained on numerous resistance layers ranged consistently between the limits $\alpha = (2.75 \text{ to } 3.2 \times 10^{-3})^{\circ} \text{C}^{-1}$, hence is lower than for pure, solid gold ($\alpha = 3.81 \times 10^{-3}^{\circ} \text{C}^{-1}$). This is probably due to impurities already contained in the gold or else in minute quantities of tungsten evaporated with it. For it is known from studies on alloys that small quantities of one of its components can cause a marked falling off of the conductivity. Aside from that the conductivity of thin layers is less than for the solid material because of the shorter mean free path lengths of the free electrons. If Matthiessen's law were applicable in this instance, the decrease in conductivity should be accompanied by a drop in the temperature coefficient.

IV. EFFECT OF THERMIC INERTIA OF RESISTANCE LAYER DURING MEASUREMENT

1. Thickness of Layer

Given the thickness of the gold and the Eloxal layer, together with the values of the material, the thermic inertia of the gold film, and hence the range of frequency within which the plug gives a record practically free from inertia, can be predicted. The thickness of the gold film can be fairly accurately computed from

1. The thickness of the evaporated layer and the electrolytically deposited volume of gold, or else from
2. The resistance and the dimensions of the layer.

To 1: The rotating motion of the tungsten spiral during the evaporating process produces circular evaporation centers as a result of the drops of gold suspended from the individual windings. But a comparative calculation indicated that the assumption of a point center of

evaporation in the axis of rotation is admissible. Under a vacuum of 10^{-4} millimeter mercury column the mean free path length of the gold atoms is much greater than the distance z_0 of the tungsten spiral from the surface to be gilded (fig. 7). Hence the evaporation can be treated as source flow and its laws applied.

With gold volume V to be evaporated as yield of the source and c_{z_0} as velocity component in the hypothetical flow distance r from the plug center perpendicular to the front surface of the plug the amount of gold allotted to the front is

$$V' = 2\pi \int_0^{r_0} r c_{z_0} dr$$

with r_0 the radius of the frontal area. The velocity c_{z_0} follows at

$$c_{z_0} = \frac{z_0 V}{4\pi (\sqrt{r^2 + z_0^2})^3}$$

Assuming the deposited gold to be of the same specific gravity as that of the solid metal, the mean thickness deposit is

$$s_1' = \frac{V}{2\pi r_0^2} \left[1 - \frac{z_0}{\sqrt{r_0^2 + z_0^2}} \right]$$

The dimensions of the gold wire were $l = 6$ mm, $d = 0.2$ mm diameter; hence a volume of $V = 0.189$ mm³, distance z_0 amounted to about 6.5 mm and $r_0 = 3.25$ mm, which gives a mean thickness of evaporated layer of

$$s_1' = 0.29 \times 10^{-3} \text{ mm}$$

to which the electrolytically precipitated volume of gold must then be added. The remainder of the calculation was

based on the numerical values obtained during the construction of a plug. The width of the spirally wound resistance layer was $b = 0.24$ mm (fig. 8), leaving a clearance of $a = 0.034$ mm between the individual windings, and making the area to be gilded approximately

$$f = \frac{b}{a + b} \pi r_o^2 = 29 \text{ mm}^2$$

The current input amounted to $Q = 1.53$ As ($i = 0.1$ ma; $\tau = 4$ hr 15 min). With gold to the amount of 0.68×10^{-3} g being precipitated, with a current of 1 As or 0.0352 mm^3 by volume with constant specific gravity, the thickness of the layer is

$$s_1'' = \frac{0.0352 Q}{f} = 1.86 \times 10^{-3} \text{ mm}$$

thus making the total thickness

$$s_1 = s_1' + s_1'' = 2.15 \times 10^{-3} \text{ mm}$$

To 2: After aging of the layer its resistance at 20°C amounted to $R = 3.81 \Omega$. The length of the layer is approximately equal to the length l of the stretched balance spring, or $l = 72$ mm for the employed spring. With the specific resistance of pure, solid gold of $\sigma = 0.023 \Omega \text{ mm}^2/\text{m}$, the deposited thickness amounts to

$$s_2 = \frac{l\sigma}{Rb} = 1.82 \times 10^{-3} \text{ mm}$$

or to

$$\bar{\sigma} = \frac{\alpha}{\bar{\alpha}} \sigma$$

if the specific resistance $\bar{\sigma}$ of the gold film is computed according to the Matthiessen law, where α , $\bar{\alpha}$ are the temperature coefficients for solid gold and gold film, respectively. The calibration curve of the plug itself afforded $\bar{\alpha} = 3.0 \times 10^{-3}^\circ \text{C}^{-1}$, with $\alpha = 3.8 \times 10^{-3}^\circ \text{C}^{-1}$; hence $\bar{\sigma} = 0.0291 \Omega \text{ mm}^2/\text{m}$ and

$$s_2 = 2.30 \times 10^{-3} \text{ mm}$$

Despite the fact that the calculation is only approximate the agreement of both results is surprisingly good; hence it may be safely assumed that the thickness of the deposit amounted to about 2×10^{-3} mm.

2. Temperature Distribution in the Resistance Layer

By means of Pfriem's theory of quasi-stationary temperature fields (reference 3) the instrumental error due to thermic inertia of the gold film and the laminated design of the plug can be computed if the thickness of the two layers and the material values are given. Lacking the material values of Eloxal, no numerically exact interpretation of this error was attempted.

Imposing a harmonic temperature oscillation with natural frequency ω on the gold film at its free surface results in a temperature distribution in the film of the form

$$\underline{T}_1 = T_{-s_1} e^{j(\omega\tau + \psi)} e^{-\varphi_1(s_1 + x)(1+j)} \frac{1 + \rho_{12} e^{2\varphi_1 x(1+j)}}{1 + \rho_{12} e^{-2\varphi_1 s_1(1+j)}},$$

$$0 \geq x \geq -s_1 \quad (1)$$

with the zero point of the coordinate system located in the contact area 1.2 of gold and eloxal layer (fig. 9). The temperature field is envisaged as being built up from a temperature wave intruding from the free surface and a wave returning from the critical area 1.2. The ratio of the amplitudes and the phase angle of the two waves at point $x = 0$ are accounted for by the reflection factor ρ_{12} . Since at this point the wave returning from the critical area 1.2 can, because of the disturbing effect of the critical area 2.3, be in or opposite phase with the wave advancing from the outside only in certain cases, the reflection factor ρ_{12} is generally a complex quantity, that is, the wave reflected at critical area 1.2 is thrown back with the phase angle of the reflection factor. It is

$$\rho_{12} = \frac{\overline{\rho'_{12}} + \rho_{23} e^{-2\varphi_2 s_2} (1 + j)}{1 + \overline{\rho'_{12}} \rho_{23} e^{-2\varphi_2 s_2} (1 + j)}$$

with

$$\overline{\rho'_{12}} = \frac{b_1 - b_2}{b_1 + b_2}; \quad \rho_{23} = \frac{b_2 - b_3}{b_2 + b_3}$$

Because of the shallow depth of penetration of the temperature waves the plug element can be treated as being of infinite length.

It denotes:

T_{-s_1} temperature amplitude at the free surface

τ time

ψ phase angle at the surface for $\tau = 0$

s thickness of layer, gold and Eloxal

$b = \sqrt{c \gamma \lambda}$ heat stress factor

$\varphi = \sqrt{\frac{\omega}{2a}}$

$a = \frac{\lambda}{c\gamma}$ temperature conduction factor

c specific heat

γ specific gravity

λ heat conduction factor

$j = \sqrt{-1}$

The numerals 1, 2, and 3 refer to the related materials (fig. 9).

To determine the instrumental error we compute the temperature difference between the two end surfaces of the resistance layer. With

$$\underline{T}_{-s_1} = T_{-s_1} e^{j(\omega\tau + \epsilon_1)}; \quad \underline{T}_0 = T_0 e^{j(\omega\tau + \epsilon_2)}$$

indicating the vectors of the temperature oscillation at the free surface and at the critical surface 1.2, the ratio of both vectors gives the vector

$$\frac{\underline{T}_0}{\underline{T}_{-s_1}} = \frac{T_0}{T_{-s_1}} e^{j(\epsilon_2 - \epsilon_1)} = p e^{j\nu}$$

Its amount represents the ratio of the temperature amplitudes and its argument ν the angle between both vectors. According to figure 10, the amount of the vector difference which is a criterion of the maximum absolute instrumental error during the cause of an oscillation is

$$|\Delta \underline{T}| = \Delta T = \sqrt{T_{-s_1}^2 + T_0^2 - 2T_{-s_1} T_0 \cos \nu}$$

With

$$T_0 = p T_{-s_1}$$

we get

$$\Delta T = T_{-s_1} \sqrt{1 + p^2 - 2p \cos \nu}$$

Confirmation of the smallness of the phase difference ν is afforded in the subsequent numerical example. For small ν it approximately affords

$$\Delta T \approx (1 - p) T_{-s_1}$$

Equation (1) gives

$$\frac{\underline{T}_0}{\underline{T}_{-s_1}} = \frac{e^{-\varphi_1 s_1} (1 + j) (1 + \rho_{12})}{1 + \rho_{12} e^{-2\varphi_1 s_1} (1 + j)}$$

for $x = 0$ and $x = -s_1$.

For convenience the complex ρ_{12} is written in the form

$$\rho_{12} = |\rho_{12}| e^{j\delta}$$

After separating denominator and numerator into real and imaginary parts by means of the Euler formula

$$e^{jw} = \cos w + j \sin w$$

ρ_{12} takes the form

$$\rho_{12} = \frac{u + jv}{x + jy} \quad \text{or} \quad \rho_{12} = \frac{\sqrt{u^2 + v^2} e^{j \tan^{-1} \frac{v}{u}}}{\sqrt{x^2 + y^2} e^{j \tan^{-1} \frac{y}{x}}}$$

with

$$u = \overline{\rho'_{12}} + \rho_{23} e^{-2\varphi_2 s_2} \cos 2\varphi_2 s_2 \quad v = -\rho_{23} e^{-2\varphi_2 s_2} \sin 2\varphi_2 s_2$$

$$x = 1 + \overline{\rho'_{12}} \rho_{23} e^{-2\varphi_2 s_2} \cos 2\varphi_2 s_2 \quad y = -\overline{\rho'_{12}} \rho_{23} e^{-2\varphi_2 s_2} \sin 2\varphi_2 s_2$$

Hence we get

$$|\rho_{12}| = \sqrt{\frac{u^2 + v^2}{x^2 + y^2}}, \quad \delta = \tan^{-1} \frac{v}{u} - \tan^{-1} \frac{y}{x}$$

$$= \tan^{-1} \frac{\frac{v}{u} - \frac{y}{x}}{1 + \frac{v}{u} \frac{y}{x}}, \quad \tan \delta = \frac{xv - uy}{ux + vy}$$

The above reflection factor therefore yields, first,

$$\rho_{12} = \frac{\overline{\rho'_{12}} + \rho_{23} e^{-2\varphi_2 s_2} \cos 2\varphi_2 s_2 - j \rho_{23} e^{-2\varphi_2 s_2} \sin 2\varphi_2 s_2}{1 + \overline{\rho'_{12}} \rho_{23} e^{-2\varphi_2 s_2} \cos 2\varphi_2 s_2 - j \overline{\rho'_{12}} \rho_{23} e^{-2\varphi_2 s_2} \sin 2\varphi_2 s_2}$$

and then

$$|p_{12}| = \sqrt{\frac{\rho'_{12}{}^2 + \rho_{23}{}^2 e^{-4\varphi_2 s_2} + 2\rho'_{12}\rho_{23}e^{-2\varphi_2 s_2} \cos 2\varphi_2 s_2}{1 + \rho'_{12}{}^2 \rho_{23}{}^2 e^{-4\varphi_2 s_2} + 2\rho'_{12}\rho_{23}e^{-2\varphi_2 s_2} \cos 2\varphi_2 s_2}}$$

$$\tan \delta = - \frac{\rho_{23}(1 - \rho'_{12}{}^2) \sin 2\varphi_2 s_2}{\rho'_{12}e^{2\varphi_2 s_2} + \rho'_{12}\rho_{23}e^{-2\varphi_2 s_2} + \rho_{23}(1 + \rho'_{12}{}^2) \cos 2\varphi_2 s_2}$$

The ratio of the amounts p and the phase difference v is computable in the same manner from the quotient of the temperature vectors. The ratio of the amplitudes is

$$p = \sqrt{\frac{1 + |p_{12}|^2 + 2|p_{12}| \cos \delta}{e^{2\varphi_1 s_1} + 2|p_{12}| \cos (2\varphi_1 s_1 - \delta) + |p_{12}|^2 e^{-2\varphi_1 s_1}}}$$

and the phase difference v follows at

$\tan v$

$$= \frac{|p_{12}| [\sin(\varphi_1 s_1 - \delta) + |p_{12}| \sin \varphi_1 s_1] - e^{2\varphi_1 s_1} [|p_{12}| \sin(\varphi_1 s_1 - \delta) + \sin \varphi_1 s_1]}{|p_{12}| [\cos(\varphi_1 s_1 - \delta) + |p_{12}| \cos \varphi_1 s_1] + e^{2\varphi_1 s_1} [|p_{12}| \cos(\varphi_1 s_1 - \delta) + \cos \varphi_1 s_1]}$$

Since the chemical values of Eloxal are not yet known, the numerical calculation of the instrumental error is being made with estimated values. The necessary data is compiled in table I.

	Gold 1	Eloxal 2 (approx.)	Aluminum 3
c [kcal/kg ^o C]	0.031	0.2	0.22
γ [kg/m ³]	19,300	4000*	2700
λ [kcal/m ^o Ch]	265	2	175
b [kcal/m ² C ^o \sqrt{h}]	400	40	322
a [m ² /s]	1.23×10^{-4}	0.69×10^{-6}	----

*See footnote on p. 16.

The reflection factors $\overline{\rho'_{12}}$ and ρ_{23} follow herefrom at

$$\overline{\rho'_{12}} = 0.82; \quad \rho_{23} = -0.78; \quad \left(\rho_{13} = \frac{b_1 - b_3}{b_1 + b_3} = 0.105 \right)$$

Figure 11 shows amount and phase of the complex reflection factor plotted against $\varphi_2 s_2$. The relation of the reflection factor with the frequency of the temperature oscillation is due to the fact that thickness s_2 appears smaller or greater corresponding to a change in wave length. The curve of quantity $|\rho_{12}|$ starts with the value ρ_{13} and approaches the reflection factor $\overline{\rho'_{12}}$ asymptotic, while phase angle δ reduces to zero in form of a markedly damped oscillation.

For a gold film of $s_1 = 2 \times 10^{-3}$ mm thickness and an Eloxal layer of $s_2 = 2 \times 10^{-2}$ mm we get

$$\varphi_1 s_1 = 3.2 \times 10^{-4} \sqrt{n} \quad \text{and} \quad \varphi_2 s_2 = 4.25 \times 10^{-2} \sqrt{n}$$

with n the frequency of the assumed harmonic temperature oscillation in Hz imposed on the gold film at its free surface. In figure 12 the curve of maximum temperature difference ΔT referred to temperature difference T_{-s_1} is shown plotted against frequency n . Putting, for instance, $T_{-s_1} = 1^\circ \text{C}$ and $n = 5000 \text{ Hz}$, would give $\Delta T \approx 2 \times 10^{-3}^\circ \text{C}$, that is, only about 2 percent of the temperature amplitude. For a frequency of that magnitude, which is equivalent to the 100th overswing in a 4-stroke-cycle engine at 6000 rpm, T_{-s_1} and consequently ΔT will be very much lower in all practicable cases. Besides, the limit of error in the evaluation of the plotted diagram is considerably higher. As the calculation indicates, the inertia of the gold deposit is practically always negligible.

*(From p. 15)

For the specific gravity of eloxal a round figure of that of crystalline aluminum oxide (corundum, ruby, sapphire) was assumed. (cf. Landolt-Börnstein Hw I 293, Eg III a 288.

V. CHANGE IN WALL TEMPERATURE DUE TO INSTALLATION OF TEST PLUG

Because of the linear heat conductivity equation the stationary field can be treated separately from the quasi-stationary. The calculation requires the knowledge of all the effects affecting the wall temperature. The foremost of these is the boundary layer, for in its existence lies the basis for the small fluctuations of the wall temperature relative to the great temperature changes in the operating room. But since correct assumptions concerning the boundary layer are hardly feasible, an accurate reduction of the recorded temperature curve to the undisturbed wall is here also impossible. On the other hand, the experimental result is in many cases not in need of a correction, because an actually existing wall temperature curve is measured so that the heat transfer coefficients can be directly obtained by known gas temperature. The heat transfer coefficient is solely dependent upon the boundary layer, but not on the material of the wall, so long as the material values of the boundary layer are not changed by the changed stationary wall temperature. A conversion of the test data dealing, say, with the reading of pressure waves in gas chambers is also superfluous, when accompanied by temperature waves of the same phase, for which this instrument is probably particularly suitable. Gas oscillations in the indicator pipe connection with their attendant incorrect if not misleading test data would be completely eliminated.

The installation of the test plug in the cast-iron wall of an internal combustion engine would result in falling off of the stationary wall temperature at the plug because of the higher heat conductivity of the aluminum. This change, however, can be but small, as the greatest heat resistance lies in the boundary layer where the heat-insulating Eloxal layer acts against it. Besides, the plug element is heated by the warmer wall material surrounding it so that, for this reason particularly, a marked assimilation with the wall temperature must take place.

In the quasi-stationary field such equalization of the two fields is no longer quite so probable. For the purpose of fixing the change in the quasi-stationary wall temperature due to the installation, the study is confined

to the case where the thickness and material values of the boundary layer remain unaltered during an operating cycle. It further is assumed that the boundary layer is sharply limited on the gas side and that the heat transport from the turbulent gas nucleus through the boundary layer to the cylinder wall is by pure heat conduction. Under these assumptions the true process in the cylinder, which mathematically is extremely difficult to essay, is reduced to an idealized stationary flow onto which a quasi-stationary temperature field is superimposed.

If the gas temperature changes harmonically with the natural frequency ω , the temperature distribution in the boundary layer follows at

$$\underline{T}_1 = T_g e^{j(\omega\tau + \psi)} e^{-\varphi_1(s_1 + x)(1+j)} \frac{1 + \rho_{12} e^{2\varphi_1 x(1+j)}}{1 + \rho_{12} e^{-2\varphi_1 s_1(1+j)}} ;$$

$$0 \geq x \geq -s_1$$

according to equation (1), the zero point of the coordinate system now being located in the critical area between boundary layer and wall: T_g is the amplitude of the gas temperature oscillation; while ρ_{12} is, in this instance, the reflection factor at the critical area between boundary layer 1 and wall 2. Denoting the material values of the plug element with 2', the temperature field in the boundary layer upstream from the plug reads:

$$\underline{T}_1' = T_g e^{j(\omega\tau + \psi)} e^{-\varphi_1(s_1 + x)(1+j)} \frac{1 + \rho_{12}' e^{2\varphi_1 x(1+j)}}{1 + \rho_{12}' e^{-2\varphi_1 s_1(1+j)}} ;$$

$$0 \geq x \geq -s_1$$

Both equations must give the gas temperatures for $x = -s_1$. It is, in fact:

$$[\underline{T}_1]_{-s_1} = [\underline{T}_1']_{-s_1} = T_g e^{j(\omega\tau + \psi)}$$

For $x = 0$ the temperature at the undisturbed wall is

$$\underline{T}_0 = T_g e^{j(\omega\tau + \psi)} e^{-\varphi_1 s_1 (1+j)} \frac{1 + \rho_{12}}{1 + \rho_{12} e^{-2\varphi_1 s_1 (1+j)}}$$

and at the plug:

$$\underline{T}_0' = T_g e^{j(\omega\tau + \psi)} e^{-\varphi_1 s_1 (1+j)} \frac{1 + \rho_{12}'}{1 + \rho_{12}' e^{-2\varphi_1 s_1 (1+j)}}$$

Then the amplitude ratio q and the phase difference ϵ for the harmonics of equal frequency can be obtained from the quotient of the two vectors: namely,

$$\frac{\underline{T}_0}{\underline{T}_0'} = \frac{1 + \rho_{12}}{1 + \rho_{12}'} \frac{1 + \rho_{12}' e^{-2\varphi_1 s_1 (1+j)}}{1 + \rho_{12} e^{-2\varphi_1 s_1 (1+j)}}$$

Having discounted the laminated structure of the plug for reasons of simplification, the two reflection factors ρ_{12} and ρ_{12}' are real quantities. The amount of the above vector is the ratio of the amplitudes

$$q = \frac{1 + \rho_{12}}{1 + \rho_{12}'} \sqrt{\frac{\rho_{12}'^2 e^{-2\varphi_1 s_1} + 2\rho_{12}' \cos 2\varphi_1 s_1 + e^{2\varphi_1 s_1}}{\rho_{12}^2 e^{-2\varphi_1 s_1} + 2\rho_{12} \cos 2\varphi_1 s_1 + e^{2\varphi_1 s_1}}}$$

and its argument the phase difference between the two wall temperature vectors. We get

$$\tan \epsilon = \frac{(\rho_{12} - \rho_{12}') \sin 2\varphi_1 s_1}{\rho_{12} \rho_{12}' e^{-2\varphi_1 s_1} + (\rho_{12} + \rho_{12}') \cos 2\varphi_1 s_1 + e^{2\varphi_1 s_1}}$$

In the reflection factors

$$\rho_{12} = \frac{b_1 - b_2}{b_1 + b_2}; \quad \rho_{12}' = \frac{b_1 - b_2'}{b_1 + b_2'}$$

b_1 is very small compared to b_2 and b_2' ; hence we can approximately write

$$q \approx \frac{b_2'}{b_2} \sqrt{\frac{\rho_{12}'^2 e^{-2\varphi_1 s_1} + 2\rho_{12}' \cos 2\varphi_1 s_1 + e^{2\varphi_1 s_1}}{\rho_{12}^2 e^{-2\varphi_1 s_1} + 2\rho_{12} \cos 2\varphi_1 s_1 + e^{2\varphi_1 s_1}}}$$

Figure 13 shows q and ϵ plotted against the dimensionless quantity $2\varphi_1 s_1$. It further shows the curves for a plug element of aluminum and porcelain to bring out the effect of the different heat stress factors on these materials. Cast iron served as wall material. With $b_1 = 0.15 \text{ kcal/m}^2 \text{ } ^\circ \text{C} \sqrt{h}$ the reflection factors read

$\rho_{12} = -0.9987$ critical layer: cast iron ($b_2 = 200 \text{ kcal/m}^2 \text{ } ^\circ \text{C} \sqrt{h}$)

$\rho_{12}' = -0.9992$ critical layer: aluminum ($b_2' = 322 \text{ kcal/m}^2 \text{ } ^\circ \text{C} \sqrt{h}$)

$\rho_{12}' = -0.9876$ critical layer: porcelain ($b_2' = 21.3 \text{ kcal/m}^2 \text{ } ^\circ \text{C} \sqrt{h}$)

With ascending frequency (φ is proportional to $\sqrt{\omega}$) the amplitude ratio q approaches a constant value asymptotically, which very approximately equals the ratio of the heat stress figures of plug and wall material, while the phase difference ϵ drops to zero in form of a markedly damped oscillation. For higher values of $2\varphi_1 s_1$ anticipated because of the marked damping effect of the boundary layer the temperature recorded at the plug would be similar to that at the undisturbed wall. Hence it would merely be necessary to multiply the temperature scale of

the measured oscillation by the value $\frac{b_2'}{b_2}$ in order to

obtain the temperature distribution at the undisturbed wall. The value of quantity $2\varphi_1 s_1$ to be expected in practical cases can be approximately ascertained if written in the form

$$2\varphi_1 s_1 = \frac{2b_1}{\frac{\lambda_1}{s_1}} \sqrt{\pi n}$$

The value of the heat stress b_1 is already known. The stationary heat transfer factor defined from boundary

layer considerations can be substituted for $\frac{\lambda_1}{s_1}$. For $\frac{\lambda_1}{s_1} = 500 \text{ kcal/m}^2 \text{ } ^\circ\text{C h}$, $n = 50 \text{ Hz} = 1.8 \times 10^5 \text{ h}^{-1}$, we get $2\phi_1 s_1 = 0.45$. The curves in figure 13, however, are practically coincident with asymptotes for this value.

For small wall temperature fluctuations the selection of plug element material alone affords the possibility of amplifying these fluctuations and hence the instrumental accuracy. Thus on the porcelain plug the recorded temperature change would be ten times greater than at the undisturbed iron wall. The extent to which the results of this calculation hold true in quasi-stationary boundary layers remains to be proved by experiments.

VI. RECORDING WALL TEMPERATURE CURVES

As stated at the beginning the test plug enables the recording of the temperature oscillations without amplification. Because of this great advantage over thermocouples the greatest value was placed on this type of measurement. Experimentally, the plotting of the diagrams by means of a thermionic valve scarcely offers material advantages over the conventional method with its required amplification while, at the same time, imposing a very much greater instrumental accuracy. Because of its extreme current sensitivity the Lindeck-Rothe compensation circuit (fig. 14) was used for the recording. It is

R resistance of the test plug variable with the temperature

R₀ a variable resistance for balancing the circuit

R_s resistance of the measuring loop

E supply of measuring current

E₀ compensation current supply

Resistances and voltages must be chosen for maximum sensitivity as will be readily apparent from the following:

According to Kirchhoff's laws, the current i_s in the loop circuit is

$$i_s = \frac{E_o (R + R_o) - E R_o}{R_o R_s + R R_o + R R_s}$$

The temperature dependence of R for a small zone can be written in the form

$$R = R' (1 + \alpha' t)$$

as the calibration curve shows only a trifling curvature. Herein R' is the plug resistance corresponding to the stationary wall temperature, α' the temperature coefficient of R referred to that temperature, and t the temperature rise above the stationary value. The sensitivity of the circuit then follows from

$$\frac{di_s}{dt} = \frac{di_s}{dR} \frac{dR}{dt}, \quad \frac{di_s}{dt} = \frac{R_o [E (R_s + R_o) - E_o R_o]}{[R_o R_s + R R_o + R R_s]^2} \alpha' R'$$

Since the resistance changes about R' are to be recorded the value of $\frac{di_s}{dt}$ substitutes for $R = R'$. In addition, i_s should be zero (by a change of R) in order to have the full deflection of the loop available to the current fluctuations. Moreover, it must have the value of (fig. 14)

$$E_o = \frac{R_o E}{R_o + R'}$$

Herewith

$$\frac{di_s}{dt} = \frac{\alpha' R_o R' E}{(R_o + R')(R_o R_s + R' R_o + R' R_s)} \quad (2)$$

Then it becomes apparent that the sensitivity can be raised by amplifying E ; but it also results in a greater flow of current through the plug resistance and an attend-

ant rise in electric energy converted to heat at the plug front. Since this heat output raises the temperature level at the wall it must be held to a minimum. Hence the various resistances must be chosen for maximum sensitivity consistent with low heat output. The latter amounts to

$$N = \frac{E^2 R'}{(R_0 + R')^2} \quad (3)$$

In view of the trifling change in the plug resistance relative to its mean value, R' can be used instead of R . Combining equations (2) and (3) by substitution of E , we get

$$\frac{N \alpha'^2}{\left(\frac{di_s}{dt}\right)^2} = \frac{(R_0 R_s + R' R_0 + R' R_s)^2}{R_0^2 R'} = \bar{R} \quad (4)$$

According to the foregoing \bar{R} must be as small as possible; it (\bar{R}) changes synonymously with R_s , hence the loop resistance must be small. The resistance of a measuring loop meets this requirement fairly closely with R_s , in general, amounting to about 1 to 5 Ω . Resistance R_0 on the other hand should be as high as possible. Assuming R_0 as given, the best plug resistance R' can be computed from equation (4); $\frac{d\bar{R}}{dR'}$ should equal 0 (minimum of \bar{R}).

$$\text{This affords } \frac{1}{R'} = \frac{1}{R_0} + \frac{1}{R_s} \quad \text{or}$$

$$R' = \frac{R_0 R_s}{R_0 + R_s} \quad (5)$$

according to which it is always necessary that $0 < R' < R_s$. The resistance of the test plug at room temperature for the manufacture can be obtained from R' by estimation of the wall temperature or from preliminary tests.

But, as seen from the circuit in figure 14, it is not possible to change the heat output N constantly

because the voltage $e' = E - E_0$ located at the plug is not uniformly variable; hence certain values of heat output are indicated. With storage batteries, which because of their voltage constancy and its small internal resistance for instrumental purposes are preferable to any other current supply, e' would be controllable only in stages of 2 V. For this reason equation (5) itself is not exactly amenable to solution because the ratio from the resistances R' and R_0 can assume certain values only.

A voltage divider bridging E and E_0 in part is impractical and may, because of its resistance, seriously impair the sensitivity of the circuit.

For calibrating the diagram the plug is replaced by a precision resistance and, starting from its value R' , (mean value of $i_s = 0$) its resistance is varied in stages by $\Delta R = \pm 0.1 \Omega$, the diagram strip being briefly illuminated after each change. The temperature changes Δt corresponding to the calibration marks can be ascertained from the analytical form of the calibration curve $R = f(t)$. Because of the very small curvature of the calibration curve we may put

$$\frac{\Delta R}{\Delta t} = \left(\frac{dR}{dt} \right)_{t'}$$

with $\left(\frac{dR}{dt} \right)_{t'}$, the pitch of calibration curve for the stationary wall temperature t' . Hence

$$\Delta t = \frac{\Delta R}{\left(\frac{dR}{dt} \right)_{t'}}$$

The instantaneous mean value of the wall temperature t' can be obtained from the resistance R' of the precision resistance and from the calibration curve.

The experiments for determining the effect of heating output on the mean wall temperature have so far produced no satisfactory result because of the impossibility of reaching a perfectly steady state in engine operation during the test. The consequence was a slow fluctuation of the mean wall temperature. But it can be safely stated that these fluctuations are very much greater than the temperature rise due to Joule effect. In the diagrams

reproduced in figures 16 to 19 the heat output amounted to about 0.3 W. But even at 0.6 W no absolutely definite effect was observable.

The diagrams were recorded by Siemens oscillograph loop type V. In the event that less sensitive loops or cathode-ray oscillographs are employed, which may be desirable in view of their more favorable frequency circle, the voltage fluctuations at the test plug must be amplified by means of thermionic valves. This should be superfluous, however, if the heat transferred from the working medium to the wall is to be ascertained from the plotted temperature distribution. During the inevitable harmonic analysis necessary, the corrections for amplitude and phase of the separate harmonics which are necessary because of the nondistortion-free plotting of the measuring loops are also readily effected.

To prove the superiority of the resistance-test plug over the conventional thermocouples even in combination with thermionic valves, the magnitude of voltage changes attainable at the test plug is briefly discussed. The bridge circuit (fig. 15) is most practical because it enables the measurement of the instantaneous mean value of the plug resistance R' in very simple fashion while possessing the same voltage sensitivity as the previously described compensation circuit. The amplifier is connected in the bridge in place of the zero instrument, so that only the voltage changes reach the first valve. Analogous to equation (4) we get

$$\frac{N \alpha'^2}{\left(\frac{de}{dt}\right)^2} = R' \left(\frac{1}{R_0} + \frac{1}{R'} \right)^2$$

with $\frac{de}{dt}$ denoting the voltage sensitivity. As is seen the resistances R' and R_0 must be chosen great in order that the expression obtains a small value. If α is the temperature coefficient of the resistance layer referred to as 20° C, the temperature coefficient α' for the mean wall temperature by linear aspect of the calibration curve is:

$$\alpha' = \frac{\alpha}{1 + \alpha (t' - 20^\circ)}$$

Assuming

$\alpha = 3.0 \times 10^{-3} \text{ } ^\circ\text{C}^{-1}$, $t' = 200^\circ \text{C}$, $R' = 200 \text{ } \Omega$,
 $R_0 = 10,000 \text{ } \Omega$, $N = 0.05 \text{ W}$ the sensitivity becomes

$$\frac{de}{dt} = 6.04 \times 10^{-3} \frac{V}{^\circ\text{C}}$$

as against $0.05 \times 10^{-3} \text{ V}/^\circ\text{C}$ with the conventional thermocouples. Even for this low heat output and for the nowise impracticably high plug resistance it afforded more than 100 times more voltage variations.

The practical use of test plugs is probably best illustrated when mounted in internal combustion engines where they are subjected to maximum demands. The plots in figures 16, 17, and 18 are records taken at the wall of the cylinder head in a two-cycle carburetor engine (DKW, water-cooled, $N_{\text{max}} = 5 \text{ hp}$ at $n = 2800 \text{ rpm}$) at 2000 rpm. The operating condition of the engine was almost the same for all records taken. The temperature distribution shown in figure 16 was measured immediately following the installation of the test plug; it reveals details very plainly, particularly the steep rise after the ignition. The records (figs. 17 and 18) taken after 1 and 10 hours of operation, respectively, manifest the increasing effect of the carbon layer deposit at the wall surface with increasing operating period. While the course in figure 17 is already perceptibly smoothened but still retains the typical marks of the first plot, the oscillation after 10 hours of operation is very markedly flattened and perfectly smooth. A subsequent test disclosed the entirety of the resistance layer, therefore the objection of an electrically conducting bridging of the individual windings through the carbon deposit is unfounded.

The damping of such a layer, even for the fundamental frequency, is extremely severe as is readily checked and increases substantially for the higher harmonics. For this very reason the refinements, especially the temperature peaks, must become lost, because they are the cause of high harmonics.

Figure 19 lastly shows the temperature distribution at the cylinder head of a four-cycle Daimler-Benz truck engine ($N_{\text{max}} = 50 \text{ hp}$ at $n = 2000 \text{ rpm}$) at 1000 rpm after about 20 hours of running. The pressure curve was plotted also.

The aim of this study was to develop the test plug to the stage where it affords an absolutely correct record of the wall temperatures. For this reason the evaluation of the test data for the purpose of determining the heat transfer has been omitted.

Translation by J. Vanier,
National Advisory Committee
for Aeronautics.

REFERENCES

1. Pfriem, H.: Zur Messung schnell wechselnder Temperaturen in der Zylinderwand von Kolbenmaschinen. Forsch. Ing.-Wes. Bd. 6, Heft 4, July-Aug. 1935, p. 195.
2. Riedel, L.: Metallwirtsch, Bd. 17, 1938, p. 1105.
3. Pfriem, H.: Beitrag zur Theorie der Wärmeleitung bei periodisch veränderlichen (quasistationären) Temperaturfeldern. Ing.-Archiv., Bd. 6, 1935, p. 97.

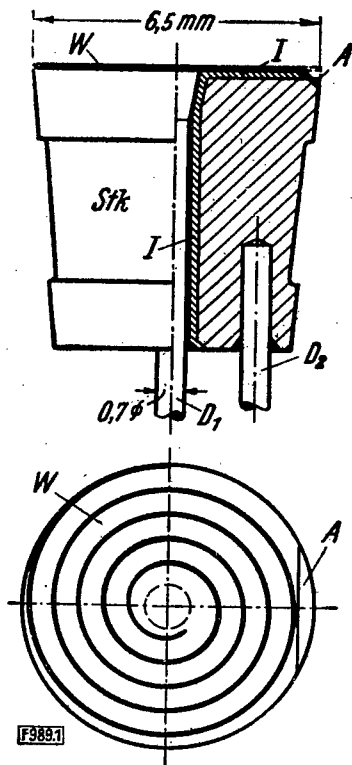
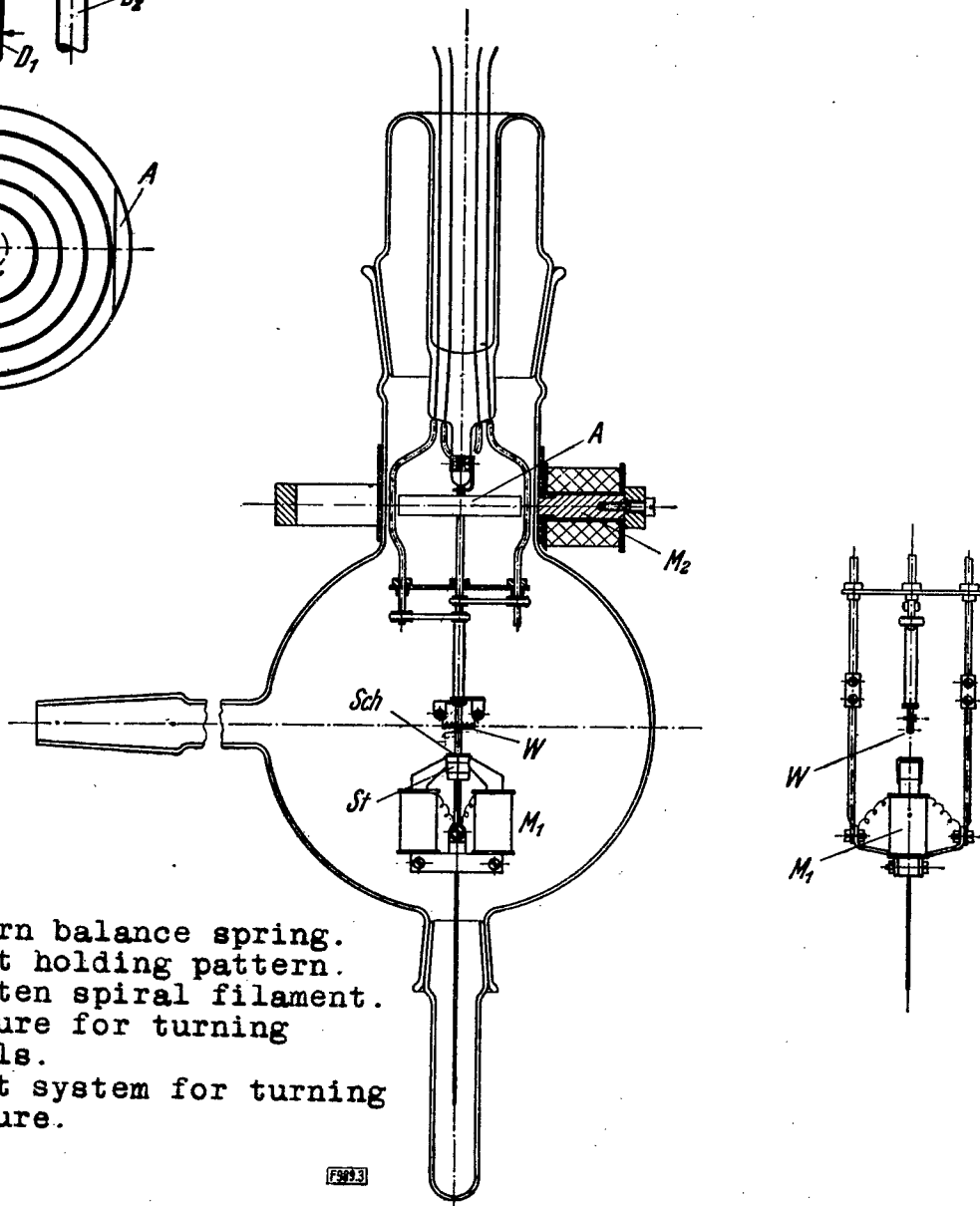


Figure 1.- Construction of measuring plug.



- St Plug.
- Sch Pattern balance spring.
- M1 Magnet holding pattern.
- W Tungsten spiral filament.
- A Armature for turning spirals.
- M2 Magnet system for turning armature.

Figure 3.- Apparatus for applying gold film.

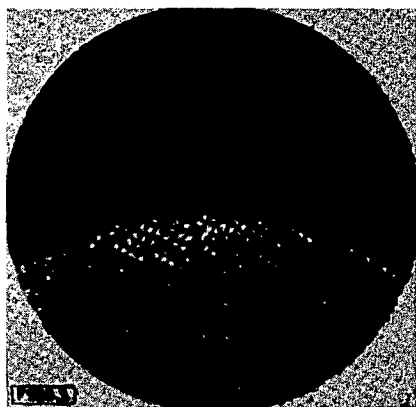


Figure 2.--Transition point from front surface of wire over eloxal layer of the hole to the plug element before deposition of resistance layer(magnified 100X).

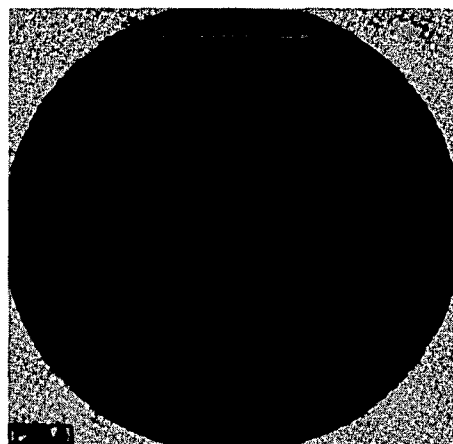


Figure 5.--Electrolytically strengthened gold film(magnification 35X).

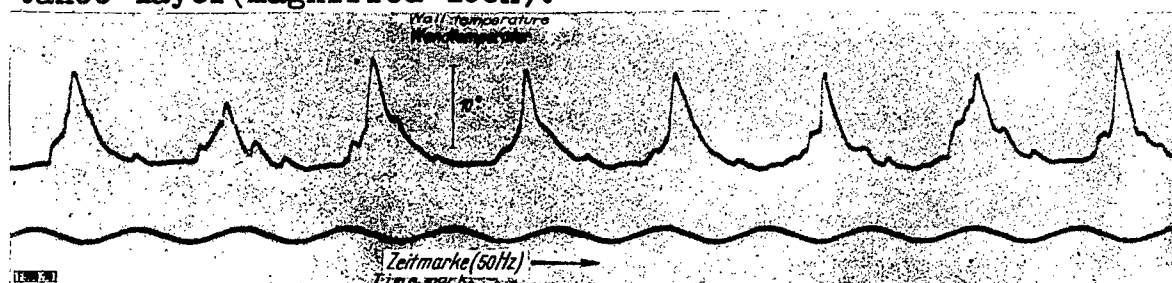


Figure 16.--Temperature distribution at wall of cylinder head, immediately after installation of measuring plug 2000 rpm; $\psi=0.6$; momentary mean wall temperature $t=204^{\circ}\text{C}$.

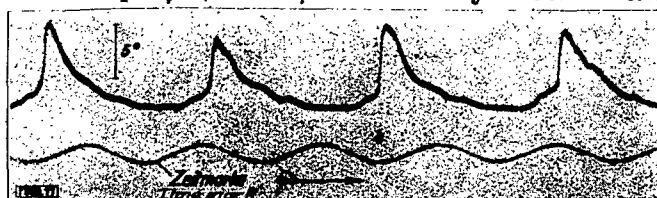


Figure 17.--Temperature distribution after 1 hour operation.



Figure 18.--Temperature distribution after 10 hours operation.

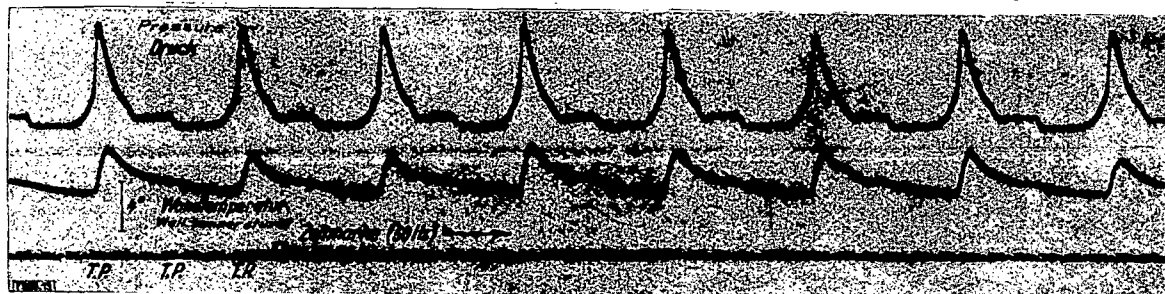


Figure 19.--Temperature distribution after 20 hours operation.

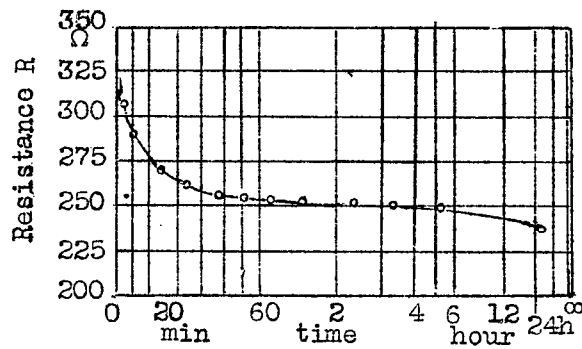


Figure 4.- Time rate of change of resistance of deposited gold film at 200° C temperature (time coordinate at hyperbolic scale.)

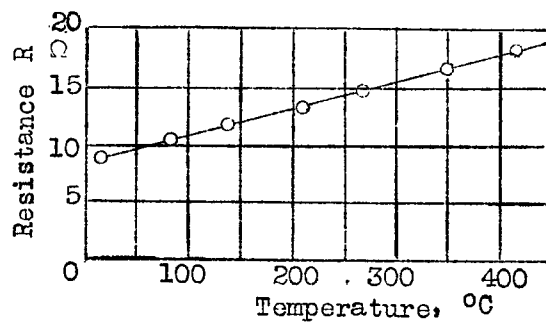


Figure 6.- Calibration curve of a plug.

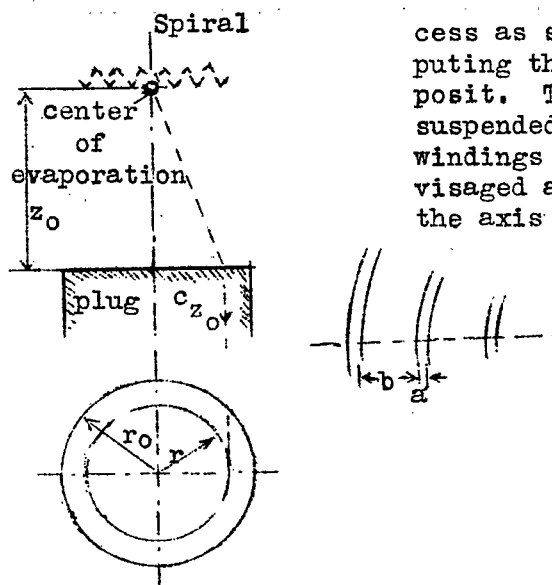


Figure 7.- Representation of gold plating process as source flow for computing the thickness of the deposit. The droplets of gold suspended from the individual windings of the spiral are envisaged as being combined in the axis of rotation.

Figure 8.- Sector of the resistance layer.

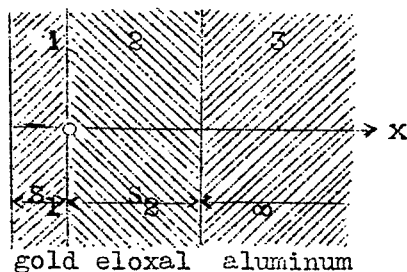


Figure 9.- Section through plug (not to scale) for computing the temperature field in the resistance layer at the surface of which ($x = -s_1$) a harmonic temperature oscillation is imposed.

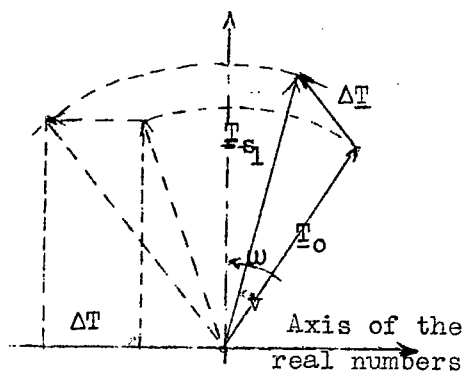


Figure 10.- Representation of temperature vectors to either side of the resistance layer in Gauss' number plane. For computing the maximum temperature difference ΔT driving an oscillation cycle.

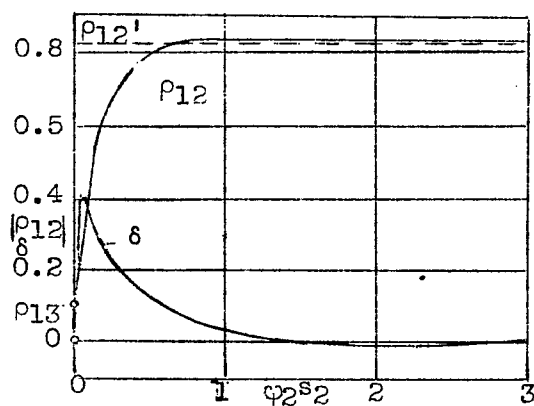


Figure 11.- Amount $|\rho_{12}|$ and phase angle δ of complex reflection factor ρ_{12} against nondimensional quantity

$$\phi_2 s_2 = \sqrt{\frac{\omega}{2a_2}} s_2$$

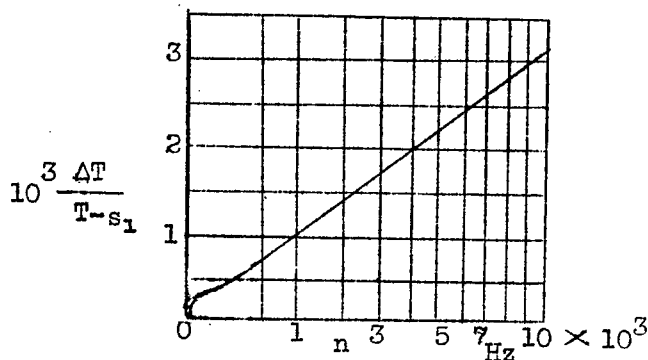


Figure 12.- Curve of maximum temperature difference ΔT between both sides of the resistance layer, referred to the amplitude $T-s_1$ of the harmonic temperature oscillation imposed at the free surface against the frequency (parabolic scale.)

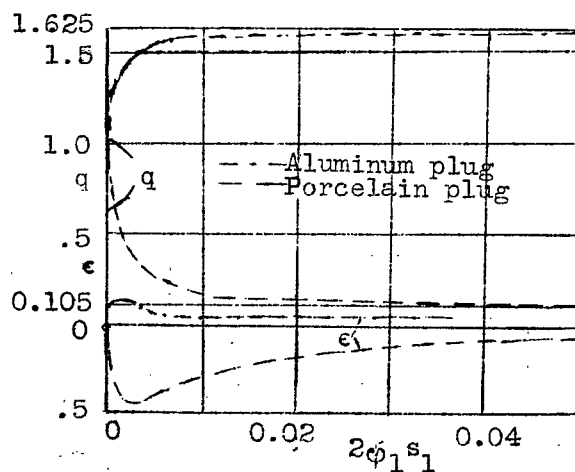


Figure 13.- Ratio of amplitudes, q , and phase difference, ϵ of the temperature oscillation occurring at iron wall and at measuring plug by harmonic change of temperature in the gas chamber against quantity $2\phi_1 s_1$

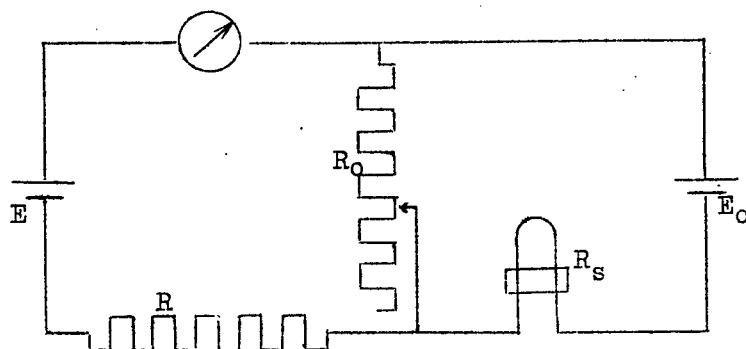


Figure 14.- Compensation circuit for direct wall temperature recording.

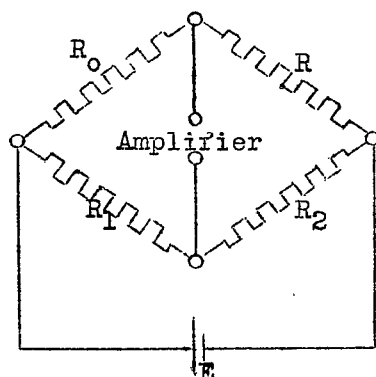


Figure 15.- Bridge circuit for recording wall temperature when amplifier is used.

LANGLEY RESEARCH CENTER



3 1176 01325 7747